Magnetron Sputtered AZO Thin Film Preparation for the Solar Cells Applications

Z. Ghorannevis[1] · E. Akbarnejad[2] · A. Salar Elahi[2] · M. Ghoranneviss[2]

Abstract Improved properties of aluminum zinc oxide (AZO) thin films deposited by the magnetron sputtering at room temperature are reported. AZO is one of the most promising transparent conducting oxide materials, which widely used in thin film solar cells. In this study the optimization process of the DC magnetron sputtered AZO films was carried out at room temperature by studying its structural, optical, electrical and morphological properties at different deposition times (5, 10, 15, 20 and 25 min) It can be utilized as a front contact for the cadmium telluride (CdTe) based thin film solar cells. The structural study shows that the preferred orientation of grains is along plane (002), with a hexagonal structure of the grains. The electrical and optical characteristics show that the films has an average transmission of 70 % and a resistivity of the order of 10^{-4} Ω cm. The morphology analysis suggests the formation of packed grains with a homogeneous surface.

Keywords AZO · TCO · Magnetron sputtering · Solar cell

1 Introduction

Aluminum doped zinc oxide (AZO) is a highly insoluble thermally stable Aluminum source suitable for glass, optic and ceramic applications. Oxide compounds are not conductive to electricity. However, certain perovskite structured oxides are electronically conductive finding usage in the solid oxide fuel cells cathode and oxygen generation systems. They are compounds containing at least one oxygen anion and one metallic cation. They are typically insoluble in aqueous solutions (water) and extremely stable making them useful in ceramic structures as simple as producing clay bowls to advanced electronics and in light weight structural components in aerospace and electrochemical applications such as fuel cells in which they exhibit ionic conductivity. Metal oxide compounds are basic anhydrides and can therefore react with acids and with strong reducing agents in redox reactions. AZO is also available in pellets, pieces, powder, sputtering targets, tablets, and nano-powder. The transparent conductive oxide (TCO) thin films are semiconductor materials with low resistivity and high transparency over a large spectral range, from visible to near infrared. The interest about these materials has been increased in the last years because they play an important role in a variety of usages such as flat panel displays, solar energy cells, and opto-electronic devices [1–5]. The TCO films must have wide band gap, low resistivity and high transmittance in the particular spectral region where the device operates. AZO is a TCO material, which shows several advantages towards the more commonly used tin-based oxide films such as wide availability of its constituent rude materials, low cost, and easier formation of its textured surface. Therefore the research in this field (the influence of the growth parameters) is intensively conducted so far [6, 7], sol–gel [8], spray pyrolysis [9], and magnetron sputtering [10]. It is known that magnetron sputtering is relatively cheap and the use of toxic gases is avoided [11–15]. In this contribution, the results of the optimization of AZO thin films deposition on soda lime glass substrates will be presented.

✉ A. Salar Elahi
Salari_phy@yahoo.com

1 Department of Physics, College of Basic Sciences, Karaj Branch, Islamic Azad University, Alborz, Iran

2 Plasma Physics Research Center, Science and Research Branch, Islamic Azad University, Tehran, Iran
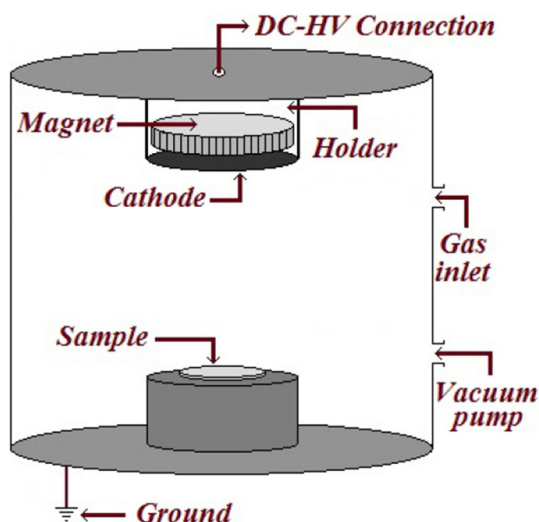
Fig. 1 Schematic of magnetron sputtering setup

Table 1 Thicknesses of the AZO thin films prepared at different deposition times

Thickness (nm)	Deposition time (min)
210	5
350	10
520	15
710	20
1150	25

This was performed by varying film thicknesses and studying its influence on the optical, structural, morphological, and electrical characteristics for achieve the highest transparency and lowest resistivity films. The outcome suggested its use as a window layer in the solar cell structure.

2 Experimental Setup

Figure 1 shows the schematic illustration of RF magnetron sputtering system. AZO thin films were produced by this setup from a 3 inch diameter target consisting of 96 % (weight) wt ZnO and 5 % wt Al₂O₃. A Dektak profilometer was also used in estimating the films thicknesses.

3 Results and Discussion

AZO thin films were prepared at different depositions times while keeping other experimental conditions constant were used for studying their physical properties such as structural, optical, electrical and morphological properties. Table 1 gives the thickness of the AZO thin films which
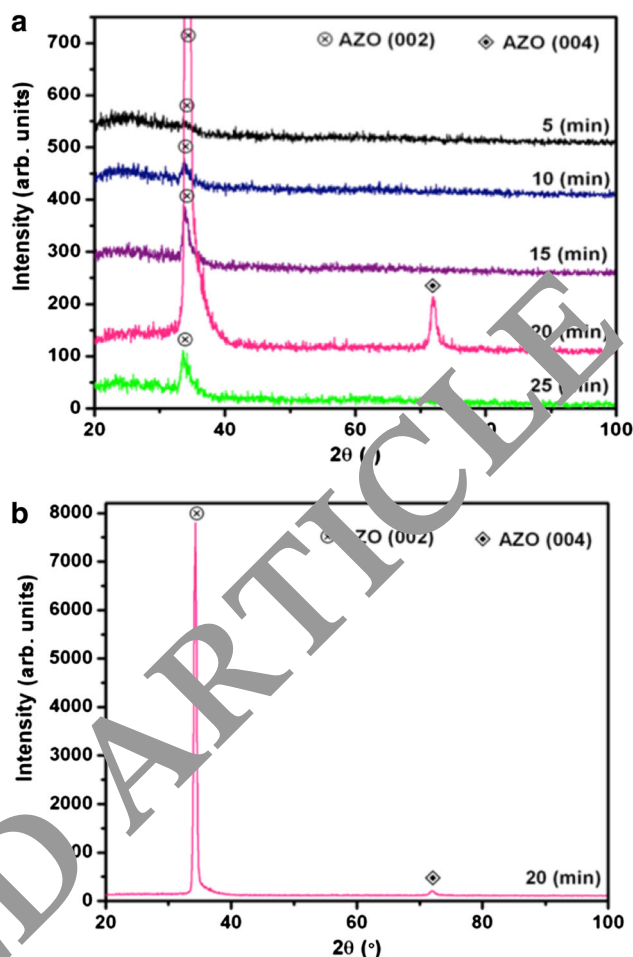

Fig. 2 XRD spectra of AZO films deposited at **a** various deposition times **b** 20 min

prepared at various deposition times of 5, 10, 15, 20 and 25 min. Figure 2a shows the X-ray diffraction (XRD) spectra of AZO films grown at various deposition times. A film, which is grown for 5 min does not shows any AZO peak, which means 5 min is not enough for formation of the crystalline AZO film. Due to increase of the deposition time, (002) peak appears. Films which grown at the deposition time of 20 min shows peak (002) with high intensity which becomes much stronger, sharper and narrower. Figure 2b shows that the (004) peak intensity is very

Table 2 Calculated grain sizes and FWHM for AZO films grown at different deposition times for (002) peaks

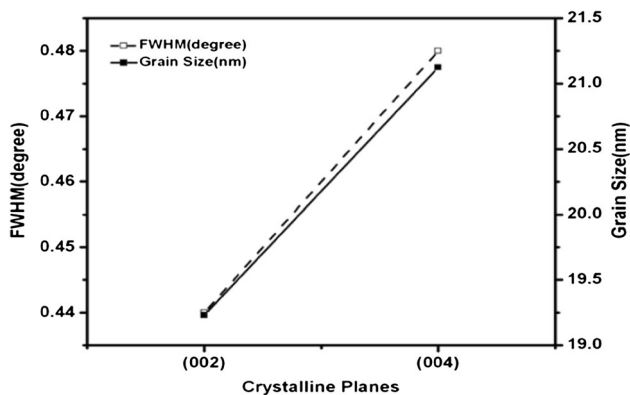| Time (min)	D-spacing (Å)	FWHM (°)	Grain size (nm)
5	2.659	0.59	14.483
10	2.656	0.96	8.725
15	2.654	0.72	11.680
20	2.618	0.44	19.231
25	2.673	0.6	14.053

Fig. 3 FWHM and grain size of (002) and (004) XRD peaks corresponding to the AZO thin film as a function of crystal planes

low in comparison with (002) peak intensity. Both peaks belong to AZO structures with two different planes. Moreover, a higher XRD intensity corresponds to improved film crystallinity for 20 min. It is clear that all the polycrystalline AZO thin films coated on the glass substrate exhibit (002) crystallographic orientation [12]. The crystalline quality of the AZO films becomes worse for higher deposition times (25 min). From the XRD data, the average size of grains of AZO film can be evaluated by Debye–Scherrer equation as follows [10]:
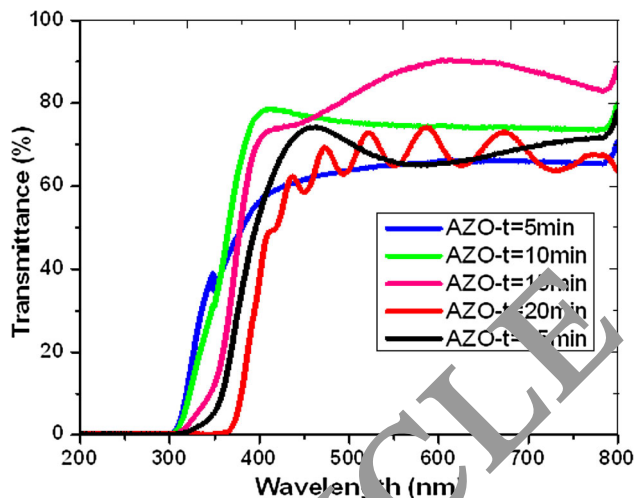

Fig. 4 The transmission over the VIS range for AZO thin film at different deposition times (color figure online)

$$\text{Grain size} = 0.9\,\lambda/\beta\cos\theta \tag{1}$$

where λ is the X-ray wavelength (0.154 nm), θ is the Bragg angle, and β is the full width at half maximum (FWHM) of the diffraction peak. The FWHM of (002) peaks are given in Table 2. The maximum grain size is around 19.231 nm for 20 min deposition time. Figure 3 shows the graph of

Table 3 Calculated crystal size and FWHM for (002) and (004) peaks for a sample prepared at 20 min deposition time

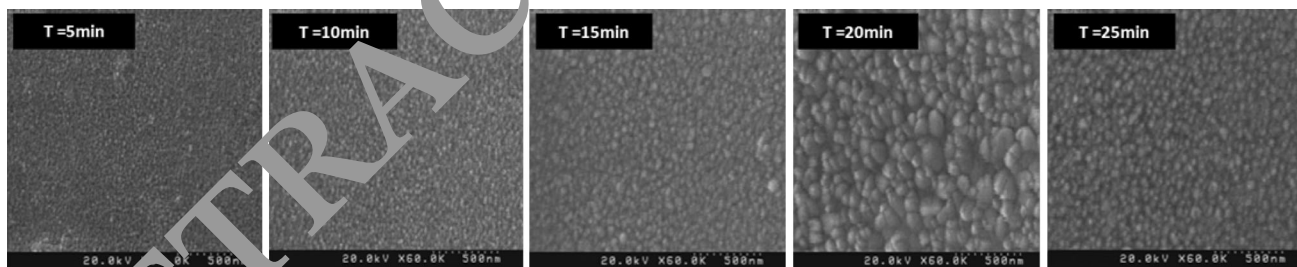| Crystal orientation	D-spacing (Å)	FWHM (°)	Grain size (nm)
(002)	2.618	0.44	19.231
(004)	1.314	0.48	21.125
Average of grain size (nm)			20.178

Fig. 5 SEM images of AZO thin films at different deposition times

Table 4 Resistivity of the thin films prepared at different deposition times

Resistivity (Ω cm)	Deposition time (min)
9.8×10^{-2}	5
3.6×10^{-2}	10
3.2×10^{-3}	15
4.1×10^{-4}	20
1.2×10^{-3}	25

Table 5 Average roughnesses of the AZO thin films deposited at different deposition times

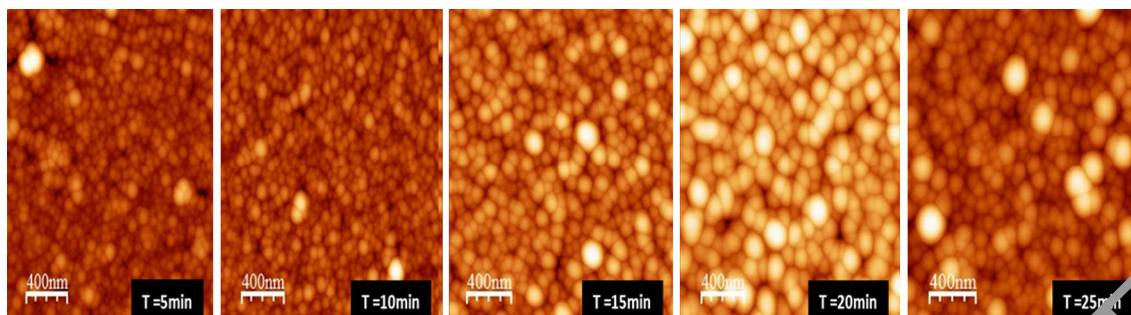| Roughness (nm)	Deposition time (min)
28.4	5
33.4	10
48.7	15
49.3	20
38.4	25

Fig. 6 AFM images of AZO thin films deposited at different deposition times

FWHM of XRD (002) and (004) peaks and grain sizes correspond to the AZO films as a function of crystal planes. It is observable that the grain size for (004) peak is larger and from Table 3 the average grain size for two AZO crystal planes is around 20 nm. Figure 4 shows the transmittance curve of AZO thin film for various deposition times [12]. As it can be seen in the Fig. 5 the film which was prepared at 20 min shows these interference fringes. Figure 5 shows the surface micrographs of films as a function of deposition time. It is observed that the deposition time has a high influence on film surface structure (Table 4). The film deposited at 20 min shows surface features of densely packed grains and grains aggregating. Figure 6 shows the AFM images of the AZO thin films deposited at various deposition times [13]. In the Fig. 6, the non-uniform surface structures of AZO thin films at various deposition times are observed. The roughnesses of the films are given in Table 5. As it can be seen the roughness increased by increase of the deposition time to 20 min correspond to the density of the thin film, which is enhanced by increasing the deposition time.

4 Conclusion

Improved properties of AZO thin films deposited by the magnetron sputtering at room temperature are reported. AZO is one of the most promising transparent conducting oxide (TCO) material, which widely used in thin film solar cells. Optical and electrical characteristics of the AZO films were optimized by increasing of the deposition time. The higher crystallinity, lower resistivity, suitable roughness and transmittance obtained for the sample prepared at 20 min deposition time.

References

1. A.R. Silva, J.O. Rossi, L.P.S. Neto, M. Ueda, Adherence enhancement of metallic film on PZT type ceramic using nitrogen plasma implantation. IEEE Trans. Plasma Sci. 42(10), 3173–3179 (2014)
2. I.B. Matveev, L.A. Rosocha, Guest editorial: classification of plasma systems for plasma-assisted combustion. IEEE Trans. Plasma Sci. 38(12), 3257–3264 (2010)
3. P.I. Vysikaylo, V.S. Mitin, A.V. Mitin, N.N. Krasnobaev, V.V. Belyaev, Theoretical model of ceramic heat sinks. IEEE Trans. Plasma Sci. 43(3), 842–849 (2015)
4. W.B. Choi, D.S. Chung, J.H. Kang, H.Y. Kim, Y.W. Jin, I.T. Han, Y.H. Lee, J.E. Jung, N.S. Lee, G.S. Park, J.M. Kim, Fully sealed, high-brightness carbon-nanotube field-emission display. Appl. Phys. Lett. 75, 3129–3131 (1999)
5. I.C. Chen, L.H. Chen, X.R. Ye, C. Daraio, S. Jin, C.A. Orme, A. Quist, R. Lal, Extremely sharp carbon nanocone probes for atomic force microscopy imaging. Appl. Phys. Lett. 88, 153102–153104 (2006)
6. S. Wong, A.T. Woolley, E. Joselevich, C.M. Lieber, Functionalization of carbon nanotube AFM probes using tip-activated gases. Chem. Phys. Lett. 306, 219–225 (1999)
7. R. Martel, T. Schmidt, H.R. Shea, T. Hertel, P. Avouris, Singleand multi-wall carbon nanotube field-effect transistors. Appl. Phys. Lett. 73, 2447–2449 (1998)
8. Q.H. Wang, T.D. Corrigan, J.Y. Dai, R.P.H. Chang, A.R. Krauss, Field emission from nanotube bundle emitters at low fields. Appl. Phys. Lett. 70, 3308–3310 (1997)
9. S. Fan, M.G. Chapline, N.R. Franklin, T.W. Tombler, A.M. Cassell, H. Dai, Self-oriented regular arrays of carbon nanotubes and their field emission properties. Science 283, 512–514 (1990)
10. C.S. Huang, C.Y. Yeh, Y.H. Chang, Y.M. Hsieh, C.Y. Ku, Q.T. Lai, Field emission properties of CNT–ZnO composite materials. Diam. Relat. Mater. 18, 452–456 (2009)
11. W.A. de Heer, A. Chatelain, D. Ugarte, A carbon nanotube field emission electron source. Science 270, 1179–1180 (1995)
12. A.G. Rinzler, J.H. Hafner, P. Nikolaev, P. Nordlander, D.T. Colbert, R.E. Smalley, L. Lou, S.G. Kim, D. Tomanek, Unraveling nanotubes: field emission from an atomic wire. Science 269, 1550–1553 (1995)
13. N. de Jonge, Y. Lamy, K. Schoots, T.H. Oosterkamp, High brightness electron beam from a multi-walled carbon nanotube. Nature 420, 393–395 (2002)
14. J. Jiao, L.F. Dong, D.W. Tuggle, C.L. Mosher, S. Foxley, J. Tawdekar, Fabrication and characterization of carbon nanotube field emitters. Mater. Res. Soc. Symp. Proc. 706, 113–117 (2002)
15. P.I. Vysikaylo, V.S. Mitin, A.V. Mitin, N.N. Krasnobaev, V.V. Belyaev, Plasma metallization coating and its adhesion to microwave transistor substrate Pt.1. methods of experimental research. IEEE Trans. Plasma Sci. 43(4), 1088–1092 (2015)